Integrated Energy & Emission Management for Heavy-Duty Diesel Engines with Waste Heat Recovery System

Frank Willems [*,**] **Frank Kupper** [*] **Robert Cloudt** [**]

[*] *Eindhoven University of Technology, Faculty of Mechanical Engineering, The Netherlands (E-mail: F.P.T.Willems@tue.nl)*
[**] *TNO Automotive, Powertrains, Helmond, The Netherlands*

Abstract: This study presents an integrated energy and emission management strategy for an Euro-VI diesel engine with Waste Heat Recovery (WHR) system. This Integrated Powertrain Control (IPC) strategy optimizes the CO_2-NO_x trade-off by minimizing the operational costs associated with fuel and AdBlue consumption. The main contribution of this work is that the effect of tailpipe emissions and WHR dynamics are included in the control design.
In a simulation study, the potential of this strategy is demonstrated over a World Harmonized Transient Cycle. These results are compared with a baseline engine control strategy. This study shows that slow WHR dynamics strongly affect the engine performance: neglecting these dynamics in the control design leads to unacceptable high tailpipe NO_x emissions. By applying the IPC strategy, an additional 2.8% CO_2 reduction is achieved within the NO_x emission limit compared to the baseline strategy.

Keywords: Energy management, engine modeling, energy storage systems, supervisory control, exhaust gas aftertreatment

1. INTRODUCTION

With the upcoming Euro-VI emission legislation, tailpipe emissions are forced towards near zero impact levels. Compared to current levels, nitrogenoxides (NO_x) and Particulate Matter (PM) emissions have to be reduced by 80% and 95%, respectively, for trucks. To meet these targets, a combination of engine measures (common rail fuel injection equipment, advanced turbocharging, Exhaust Gas Recirculation (EGR)) and aftertreatment systems (soot filters, catalysts) will be applied.

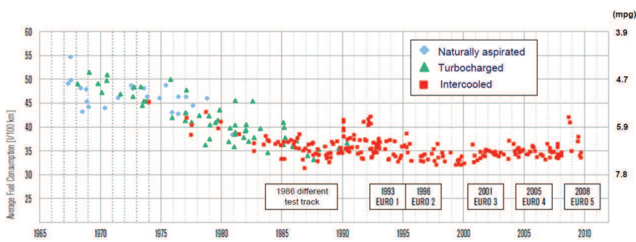

Fig. 1. Historic fuel consumption for 40 ton trucks (ACEA, 2011)

As illustrated in Figure 1, it has been increasingly challenging to keep the fuel consumption (and thus CO_2 emission) around the current level for each emission phase. However, driven by concerns around global warming and energy security, attention for heavy-duty applications currently also moves towards CO_2 emission reduction. On top of the current targets for pollutants, up to 20% CO_2 reduction has to be realized in 2020 compared to the 2010 standards in the US (EPA, 2011). Similar measures are discussed now in Europe (ACEA, 2008).

For distribution trucks, garbage trucks and city buses, hybrid-electric drivetrains attract much attention to reduce CO_2 emissions. These drivetrains are less effective for long haul truck applications. In these cases, Waste Heat Recovery (WHR) seems a very promising technology (Nelson, 2009; Park et al., 2011; Bredel et al., 2011); in WHR systems, energy is recovered from heat flows, as illustrated in Figure 2.

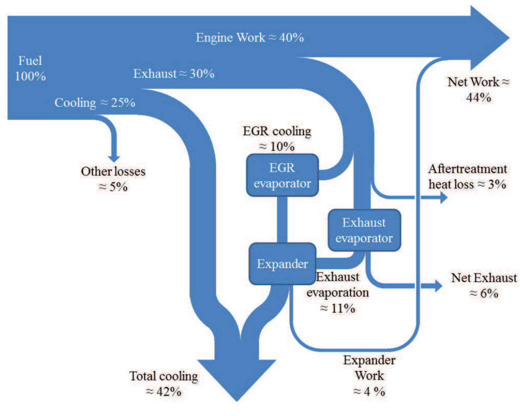

Fig. 2. Energy flows for engine with WHR system.

Up to 6% fuel consumption reduction has been demonstrated (Bredel et al., 2011; Park et al., 2011). However, WHR control studies mainly focus on low level WHR system control, see *e.g.*, (Quoilin et al., 2011; Howell et al., 2011). Only a very few studies concentrate on energy management strategies for the complete engine (Hounsham et al., 2008). These studies do not deal with the impact of the WHR system on emissions.

In this study, a cost-based optimization strategy is presented that explicitly deals with the requirements for CO_2 and pollutant emissions (Kupper, 2012). This strategy integrates energy and emission management and exploits the interaction between engine, aftertreatment and WHR system: Integrated Powertrain Control (IPC). Contrary to Willems et al. (2012), the WHR system dynamics are dealt with in both the simulation model and the control strategy. It is shown that this is required in order to optimize the overall performance.

This work is organized as follows. First, the studied powertrain and applied models are presented in Section 2. Section 3 discusses the developed IPC strategy. For a World Harmonized Transient Cycle, the results of this IPC strategy are compared with the results of a baseline engine control strategy in Section 5. Finally, conclusions are drawn and directions for future research are sketched.

2. SYSTEM DESCRIPTION

Figure 3 shows a scheme of the examined engine platform. It is based on a 6 cylinder, 13 liter, 340 kW Euro-VI diesel engine, which is equipped with a cooled Exhaust Gas Recirculation (EGR) system and a turbocharger with Variable Turbine Geometry (VTG). Furthermore, an exhaust gas aftertreatment system is installed. This system consists of a Diesel Oxidation Catalyst (DOC), a Diesel Particulate Filter (DPF) and an urea-based Selective Catalytic Reduction (SCR) system.

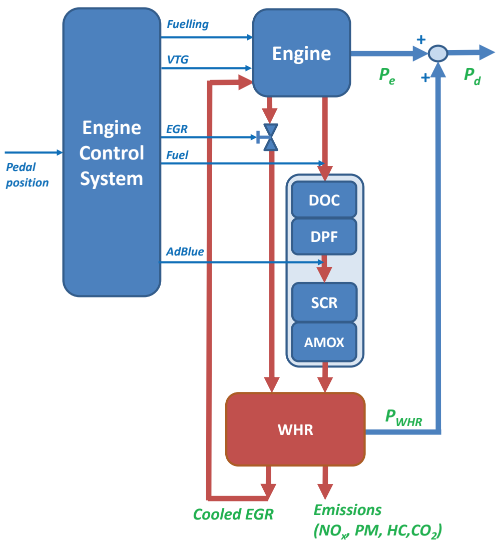

Fig. 3. Scheme of Euro-VI engine with WHR system

The DPF system removes the particulates from the exhaust flow. To avoid clogging of the filter, fuel is periodically injected upstream of the DOC. As a result, the exhaust gas temperature is raised, such that the trapped particulates are oxidized. The remaining NO_x emissions downstream of the DPF system are converted into harmless products (nitrogen and water) over the 32.6 liter Cu-Zeolite SCR catalyst. For this catalytic process, ammonia (NH_3) is required. This is partly formed upstream of the catalyst by decomposition of the injected aqueous urea solution (tradename: AdBlue) in the hot exhaust gases. Further decomposition takes place in the SCR catalyst. To avoid unacceptable NH_3 slip, an ammonia oxidation catalyst (AMOX) is installed.

For this study, the Euro-VI engine is extended with a Waste Heat Recovery (WHR) system. This system is based on a Rankine cycle, in which the recovered thermal energy is converted into mechanical energy in the expander. Similar to Howell et al. (2011), this WHR system is characterized by:

- Thermal energy is recovered from both EGR and exhaust gas flow;
- Expander is directly connected to the crank shaft.

The following sections give a description of the applied simulation and control model.

2.1 Simulation model

Engine To describe the behavior of the exhaust gas mass flow $\dot{m}_{exh}$, exhaust gas temperature T_{exh} and engine out NO_x mass flow $\dot{m}_{NOx}$, engine maps are applied. These four-dimensional maps $f(N_e, \tau_e, u_{EGR}, u_{VTG})$ are constructed using a validated mean-value engine model. For varying combinations of EGR valve position u_{EGR} and VTG position u_{VTG}, the fuel mass $\dot{m}_f$ is varied such that the requested torque $\tau_{d,req} = \tau_e$ is realized (with constant engine speed N_e [rpm]). Note that these maps are determined for the engine without WHR system.

Aftertreatment system A high fidelity aftertreatment model is implemented to simulate the DOC/DPF and SCR system. This modular model is built up using one-dimensional submodels of a pipe with urea decomposition, pre-oxidation catalyst (DOC), DPF, SCR catalyst, and ammonia oxidation (AMOX) catalyst. All catalyst models are based on first principle modeling and consist of mass and energy balances. By dividing the catalyst in various segments, these validated models describe the spatial distribution of pressure, temperature and chemical components. Further details on the model approach and SCR model can be found in Willems and Cloudt (2011).

Waste Heat Recovery system In this study, the WHR system dynamics are modeled by a first order model with constant overall efficiency η_{WHR} (assuming ideal low-level WHR controls). This is inspired by the observed thermal dynamics in various applications.

The thermal energy is recovered from both the EGR and exhaust gas flow:

$$\dot{Q}_{WF} = G(s) \cdot \left(\dot{Q}_{EGR,g} + \dot{Q}_{exh,g}\right) \qquad (1)$$

where:

$$G(s) = \frac{1}{\alpha_{WHR}s + 1} \qquad (2)$$

and the EGR and exhaust heat flows are given, respectively, by:

$$\dot{Q}_{EGR,g} = \dot{m}_{EGR} \cdot c_{p,EGR} \cdot (T_{EGR,in} - T_{EGR,out})$$
$$\dot{Q}_{exh,g} = \dot{m}_{exh} \cdot c_{p,exh} \cdot (T_{SCR} - T_{tp})$$

This thermal energy is finally converted into mechanical power at the expander shaft:

$$P_{WHR} = (1 - u_{WHR}) \cdot \eta_{WHR} \cdot \dot{Q}_{WF} \tag{3}$$

In case no power is requested from the WHR system (*e.g.*, during braking or gear shifting), the actuator u_{WHR} is activated: $u_{WHR} = 1$ if $\tau_{d,req} \leq 0$.

In all simulations, a constant overall efficiency $\eta_{WHR} = 0.15$, time constant $\alpha_{WHR} = 60$ [s], and a constant post-WHR exhaust gas temperature T_{tp} =110 [^oC] are applied.

2.2 Control model

This section presents the control model that is applied in the optimal control strategy in Section 3. For real-world implementation, this simplified model has to represent the main system characteristics and has to be evaluated in real-time. Compared to the simulation model, the main difference lies in the description of the aftertreatment; identical engine maps and WHR system model are applied.

The thermal behavior of the total DOC-DPF-SCR system is described by two coupled differential equations, see Eq. (4). Note that the DOC-DPF system behavior is lumped in one equation. For the SCR conversion efficiency η_{SCR}, a set of three stationary maps is used, which are determined for different pre-SCR concentration ratios C_{NO_2}/C_{NO_x} (0, 0.5, 1.0) and a specified ammonia slip level. As illustrated in Figure 4, the individual SCR efficiency maps depend on the average SCR catalyst temperature T_{SCR} [^oC] and space velocity SV [1/hr]:

$$SV = 3600 \cdot \frac{\dot{m}_{exh}}{\rho_{exh} V_{cat}}$$

with normal condition exhaust gas density ρ_{exh} [g/m^3] and SCR catalyst volume V_{cat} [m^3]. Using the predicted C_{NO_2}/C_{NO_x} ratio from a stationary DOC efficiency map, the NO_x conversion efficiency η_{SCR} is computed by interpolation.

In summary, the control model is written in state space form $\dot{x} = f(x)$:

$$\dot{x} = \begin{bmatrix} c_1 \cdot \dot{m}_{exh} \left[T_{exh} - T_{DOC}\right] \\ c_2 \cdot \dot{m}_{exh} \left[T_{DOC} - T_{SCR}\right] - c_3 \left[T_{SCR} - T_{amb}\right] \\ \dot{m}_{NOx} \left[1 - \eta_{SCR}(T_{SCR}, SV, C_{NO_2}/C_{NO_x})\right] \end{bmatrix} \tag{4}$$

with state variables:

$$x = \begin{bmatrix} T_{DOC} \\ T_{SCR} \\ m_{NOx,tp} \end{bmatrix} = \begin{bmatrix} \text{DOC catalyst temperature} \\ \text{SCR catalyst temperature} \\ \text{NO}_\text{x} \text{ tailpipe emission} \end{bmatrix}$$

The applied model parameters are specified in Table 1.

Table 1. Control model parameters

Constant	Unit	Definition	Value
c_1	kg^{-1}	$\frac{c_{p,exh}}{C_{DOC}}$	0.1163
c_2	kg^{-1}	$\frac{c_{p,exh}}{C_{SCR}}$	0.0512
c_3	$s \cdot kg^{-1}$	$\frac{h}{C_{SCR}}$	1.0000

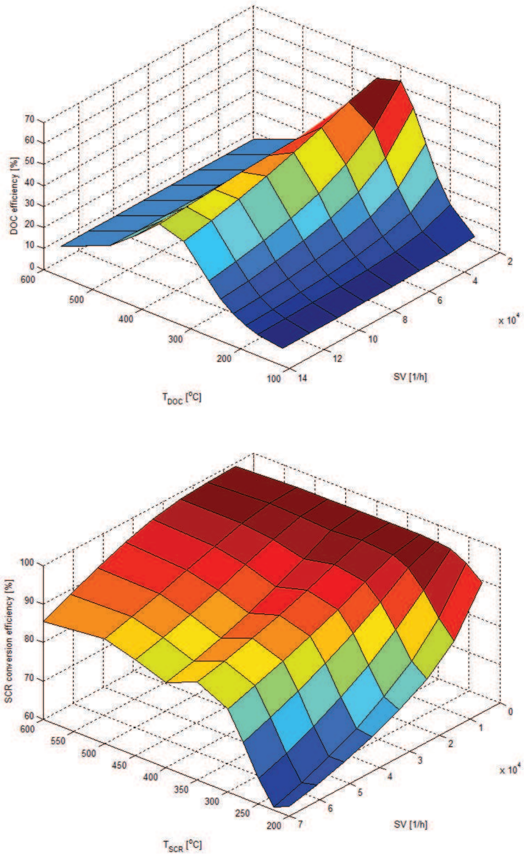

Fig. 4. DOC efficiency map C_{NO_2}/C_{NO_x} (top) and SCR efficiency map for $C_{NO_2}/C_{NO_x} = 0.5$ (bottom)

3. CONTROL STRATEGY

Figure 5 shows a scheme of the proposed engine control system. Main goal of this control system is to determine the settings for the control inputs:

$$u^T = [\dot{m}_f \ \dot{m}_a \ u_{EGR} \ u_{VTG}],$$

such that fuel consumption is minimized within the constraints set by emission legislation. By assuming ideal torque management, the requested engine torque is determined from:

$$\tau_{e,req} = \tau_{d,req} - \tau_{WHR} \tag{5}$$

with the actual produced WHR torque τ_{WHR} [Nm] available from measurements or estimation.

To satisfy these requirements, the Integrated Powertrain Control (IPC) approach, which is introduced in (Willems and Foster, 2009), is followed. This model-based approach integrates energy and emission management by exploiting the synergy between engine, WHR and aftertreatment

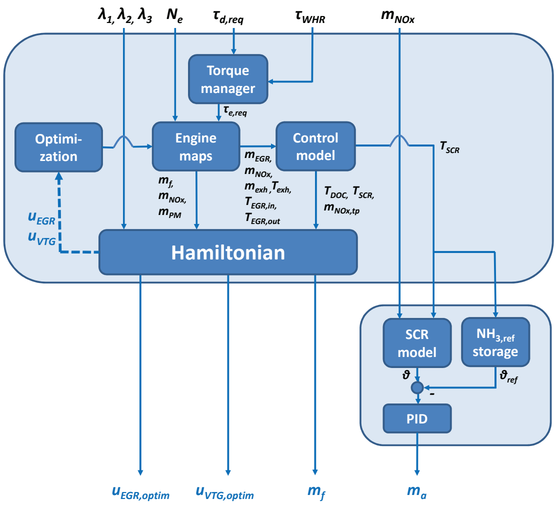

Fig. 5. Scheme of the engine control system

system. The developed IPC strategy is compared with a baseline engine control strategy, for reference. The examined control strategies are described below.

3.1 Optimization problem

Following the IPC approach, the studied control problem is formulated in the optimal control framework. We propose to minimize the total operational costs associated with fuel, AdBlue consumption and active DPF regeneration. Consequently, the following objective function is defined:

$$\min_{u_{EGR},u_{VTG}} \int_0^{t_e} w(N_e,\tau_d)\cdot[\pi_f\dot{m}_f+\pi_a\dot{m}_a+\pi_{PM}\dot{m}_{PM}]\,dt \quad (6)$$

subject to:

$$\frac{\int_0^{t_e}\dot{m}_{NOx\_tp}\,dt}{\int_0^{t_e}\frac{P_d}{3.6\times10^6}\,dt} \le Z_{NOx}\ \text{(tail-pipe NO}_x\text{ limit)} \quad (7)$$

with diesel price $\pi_f = 1.34\times10^{-3}$ [Euro/g], AdBlue price $\pi_a = 0.50\times10^{-3}$ [Euro/g], and fuel costs associated with active DPF regeneration per gram of accumulated soot $\pi_{PM} = 7.10\times10^{-2}$ [Euro/g].

Assuming that all injected urea decomposes in ammonia and is available for NO_x conversion, the desired AdBlue dosage $\dot{m}_a$ [g/s] in Eq.(6) is determined from:

$$\dot{m}_a = c_5\cdot\eta_{SCR}(T_{SCR},SV,C_{NO_2}/C_{NO_x})\cdot\dot{m}_{NOx} \quad (8)$$

where $c_5 = 2.0067$ and $\dot{m}_{NOx}$ [g/s] is the engine out NO_x emission. With the weighting function $w(N_e,\tau_d)$, it is aimed to capture the desired performance independent of the applied test cycle, see also Section 4.

3.2 IPC strategy

For this optimization problem, Pontryagin's Minimum Principle is applied to find an optimal solution, see, *e.g.*, Geering (2007). Accordingly, a Hamiltonian is formulated which entails the objective function from Eq.(6) augmented with Lagrange multipliers λ and the state dynamics $f(x)$ from Eq.(4):

$$H = w(N_e,\tau_d)\cdot[\pi_f\dot{m}_f+\pi_a\dot{m}_a+\pi_{PM}\dot{m}_{PM}]+\lambda^T f(x) \quad (9)$$

These Lagrange multipliers represent equivalence price parameters and have the following interpretation:

- λ_1 represents a cost-equivalent parameter for a DOC/DPF temperature rise of 1 $[^oC]$ within 1 [s]. A larger value will result in higher T_{DOC};
- λ_2 represents a cost-equivalent parameter for a SCR temperature rise of 1 $[^oC]$ within 1 [s]. By increasing its value, a better heat transfer between DOC/DPF and SCR can be achieved, and so a better SCR conversion efficiency;
- λ_3 takes into account the accumulated tailpipe NO_x emissions. A higher value will more penalize the raw engine out NO_x emissions;

Two necessary conditions for optimality of the solution u can be formulated:

$$-\frac{\partial H}{\partial x} = \dot{\lambda} \quad (10)$$

$$\frac{\partial H}{\partial u} = 0 \quad (11)$$

From these conditions, it is easily seen that λ_3 remains constant for the optimal solution, and only depends on its initial conditions $\lambda_3(0)$. However, a solution for λ_1, λ_2, u_{EGR} and u_{VTG} is intractable.

As we want to use the presented systematic framework, the pragmatic approach that is described in Cloudt and Willems (2011) is followed; the course of λ_1 and λ_2 are determined by a heuristic, postulated rule parameterized by λ_T, ΔT_1 and ΔT_2. This approach is illustrated in Figure 6. The effort to heat up the aftertreatment system is assumed to be proportional to the SCR inefficiency $1-\eta_{SCR}$. When T_{DOC} is lower or marginally higher than T_{SCR}, it seems better to invest in raising the engine-out exhaust temperature rather than promoting heat convection from DOC/DPF to SCR (high λ_1). The converse holds when $T_{DOC} \gg T_{SCR}$ (high λ_2).

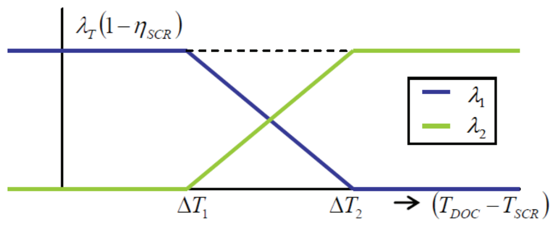

Fig. 6. Rule for λ_1 and λ_2 (Cloudt and Willems, 2011)

This sub-optimal controller is implemented in the presented simulation model. At every time step over the studied test cycle, the Hamiltonian (9) is numerically optimized on-line using a bounded 2D gradient descent method for the specified set of Lagrange multipliers λ. In Section 4, the off-line calibration of these multipliers is discussed.

3.3 Baseline strategy

For the baseline engine control strategy, we mimic a state-of-the-art air management strategy for a standard Euro-VI engine configuration (without WHR system). This strategy is characterized by switching between two control modes:

(1) **Thermal management mode (M1)** for rapid heat-up of the aftertreatment system ($T_{SCR} < 200$ [^oC]);
(2) **Low** NO_x **mode (M2)** for normal operation ($T_{SCR} \geq 250$ [^oC]).

A fundamental difference with the IPC strategy is that the baseline strategy relies on fixed control settings (u_{EGR}, u_{VTG}) for each engine operating point (N_e, τ_e). For both modes, these settings are pre-determined in an off-line optimization procedure, which is often based on stationary test conditions.

As we want to use the same control structure for both strategies in simulations, two different sets of constant λ are used for the control modes (see Table 2). As engine calibration is mainly optimized using steady state measurements, anticipated steady-state T_{DOC} and T_{SCR} values from the engine maps are used in the Hamiltonian to evaluate the SCR efficiency maps.

4. CONTROL DESIGN

This section discusses the control design procedure for the applied strategies. An overview of the selected control parameters is given in Table 2.

Table 2. Selected control parameters

Control strategy	Control parameters $-\lambda_{1,M1}$	$\lambda_{1,M2}$	λ_2	λ_3
Baseline(-WHR)	$2.0 \cdot 10^{-5}$	0	0	$6.8 \cdot 10^{-3}$
Recal-WHR cal1	$1.2 \cdot 10^{-5}$	0	0	$3.9 \cdot 10^{-3}$
Recal-WHR cal2	$1.2 \cdot 10^{-5}$	0	0	$4.5 \cdot 10^{-3}$
	ΔT_1	ΔT_2	$-\lambda_T$	λ_3
IPC-WHR cal1	84.0	101.2	$2.5 \cdot 10^{-6}$	$2.1 \cdot 10^{-4}$
IPC-WHR cal2	20.5	156.3	$5.2 \cdot 10^{-6}$	$1.8 \cdot 10^{-4}$

4.1 Baseline strategy with WHR system

For the baseline strategy, the control design boils down to the determination of:

- **Air management**: engine maps for EGR valve and VTG settings by specifying the corresponding λ set for the control modes;
- **SCR control**: θ_{ref} map and PID-control settings.

These controllers have to be designed, such that the specified engineering target of 0.41 g/kWh is met. To realize this, a NO_x emission budget and averaged SCR conversion efficiencies η_{SCR} are specified for both cold and hot World Harmonized Transient Cycle (WHTC), see Table 3.

Air management Following Cloudt and Willems (2011), two different sets of constant (λ_1, λ_3) are determined to specify the control modes of the baseline controller. For the low NO_x mode, $\lambda_{1,M2}$ and λ_2 are set to zero (no promotion of aftertreatment heat up), while λ_3 is tuned such that the engine out NO_x emission target is reached over the WHTC. For the thermal mode, λ_3 is kept unchanged, whereas $\lambda_{1,M1}$ is tuned to get maximal T_{exh} increase within the targets set for engine out NO_x emission. This baseline Euro-VI case is the reference for the other studied strategies.

Table 3. Emission targets for control design

Cycle	$NO_{x,eo}$ (g/kWh)	η_{SCR} (%)	Weighting (%)	$NO_{x,tp}$ (g/kWh)
Cold WHTC	3.5	80	16	0.112
Hot WHTC	3.5	90	84	0.294
Weighted WHTC				0.406

The baseline engine controller is also applied to the engine with WHR system (referred to as *Baseline-WHR*). In this case, the applied engine maps and controller settings are identical to the baseline strategy. However, the main difference is the implemented torque manager: the requested torque $\tau_{d,req}$ is realized by an ideal torque split, as described by Eq. (5). This means that, compared to the baseline case, the engine will run in different operating points depending on the power delivered by the WHR system.

In the baseline-WHR case, the controller does not account for the effect of the WHR system on emissions. This can lead to relatively large deviations from the targets set for emissions. Consequently, this controller is tuned such that powertrain with WHR system is closely meeting the 0.41 g/kWh target again. This case is referred to as Recal-WHR and the corresponding new set (λ_1, λ_3) can be found in Table 2. Note that a distinction is made between the case where WHR dynamics $G(s)$ are neglected (*Recal-WHR cal1*) and are included (*Recal-WHR cal2*) in the control design.

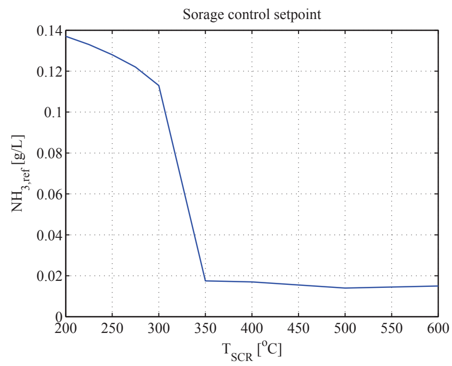

Fig. 7. Reference ammonia storage θ_{ref}

Low-level SCR control For AdBlue dosing control, a model-based ammonia storage controller is applied. This low-level controller is based on a SCR catalyst model, which estimates the ammonia storage θ from SCR catalyst temperature T_{SCR} and pre-SCR NO_x emissions $\dot{m}_{NOx}$ in real-time. This estimated value is compared with a reference value θ_{ref}. The difference is fed to the PID controller. By controlling θ, we aim to achieve high NO_x

conversion efficiency and avoid excessive NH_3 slip in case of a sudden temperature increase.

For the standard Euro-VI engine with baseline strategy, the static map $\theta_{ref}(T_{SCR})$ is calibrated, such that tailpipe NO_x emission meets the specified standards over the studied World Harmonized Transient Cycle (WHTC). Furthermore, cycle-averaged and peak tailpipe NH_3 emissions are kept within 10 and 25 [ppm], respectively. The applied θ_{ref} map is shown in Figure 7. This SCR control calibration is used in all simulations.

4.2 IPC strategy

For the IPC strategy, the following set of control parameters have to be specified:

- Weighting function $w(N_e, \tau_d)$;
- Lagrange multipliers and their related variables: $\Delta T_1, \Delta T_2, \lambda_T$ and λ_3

Weighting function Figure 8 shows the applied weighting function $w(N_e, \tau_d)$. For the studied cold and hot WHTC, typical operating points corresponding to high way driving are weighted more heavily, such that more attention is paid to minimize the operational costs during long haul driving conditions.

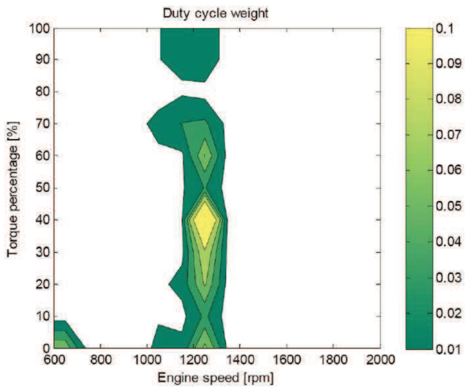

Fig. 8. Weighting function $w(N_e, \tau_d)$ (Cloudt and Willems, 2011)

Lagrange multipliers To minimize the objective function over the studied cycle, a numerical minimization method is applied. This method aims to find the control parameters $\Delta T_1, \Delta T_2, \lambda_T$ and λ_3 that minimize the operational costs over the hot WHTC cycle, while the weighted cold/hot NO_x emissions stay within the specified limits. For this purpose, the cumulative cycle costs are evaluated. By applying the Nelder-Mead simplex method, the optimal set of control parameters is found that corresponds to the lowest costs over the studied duty cycle.

Similar to the Recal-WHR strategy, two cases are examined: first, as in Willems et al. (2012), the WHR dynamics are neglected (*IPC-WHR cal1*) in the control design. In the second case, the controller is designed for the WHR system with slow dynamics (*IPC-WHR cal2*). The resulting values are listed in Table 2.

5. SIMULATION RESULTS

To evaluate the performance of the proposed controllers, simulations are done over the World Harmonized Transient Cycle (WHTC), as shown in Figure 9. This cycle specifies the requested engine speed N_e and torque $\tau_{d,req}$. Three parts can be distinguished: urban driving conditions (0-900 [s]), rural driving conditions (900-1380 [s]), and highway driving conditions. As we focus on Euro-VI emission targets, results are generated for both cold and hot cycle conditions. In case of a cold cycle, the initial SCR catalyst temperature is set to 20 [^oC]; engine heat up is not modeled yet. In all simulations, $\alpha_{WHR} = 60[s]$ is applied. It is noted that this study focuses on relative changes, since an accurate WHR model is currently lacking.

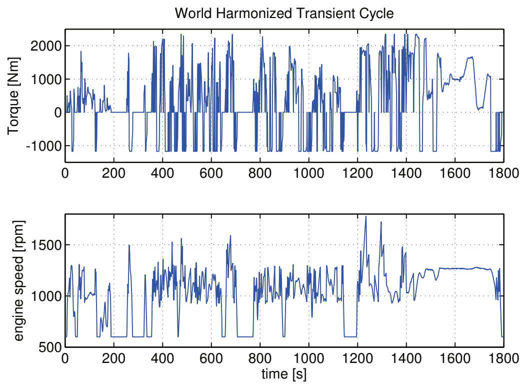

Fig. 9. World Harmonized Transient Cycle

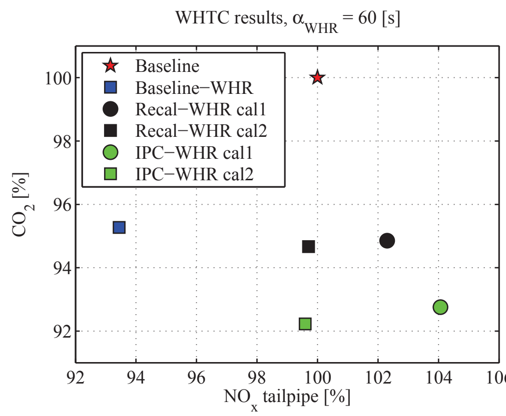

Fig. 10. CO_2-NO_x tradeoff for WHTC

Figure 10 summarizes the results for the studied control strategies. It shows the trade-off between the cycle-averaged CO_2 and NO_x emissions. For reference, the results are shown for the conventional Euro-VI engine without WHR system (*Baseline*). From this figure, it is concluded that the engine performance significantly degrades when the WHR dynamics are neglected in the control design (*cal1*); especially, tailpipe NO_x emissions reach unacceptable levels, see also Table 4. This effect is more prone for WHR systems with increasing α_{WHR} (Kupper, 2012).

The effect of the WHR dynamics is illustrated in Figure 11 for the IPC case. With increasing time constant α_{WHR},

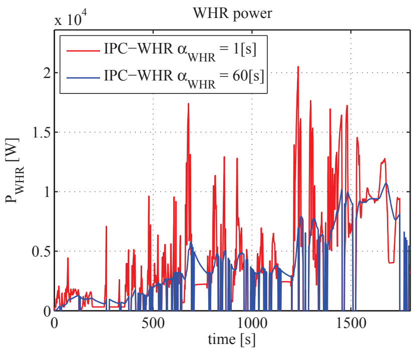

Fig. 11. Effect of α_{WHR} on P_{WHR}

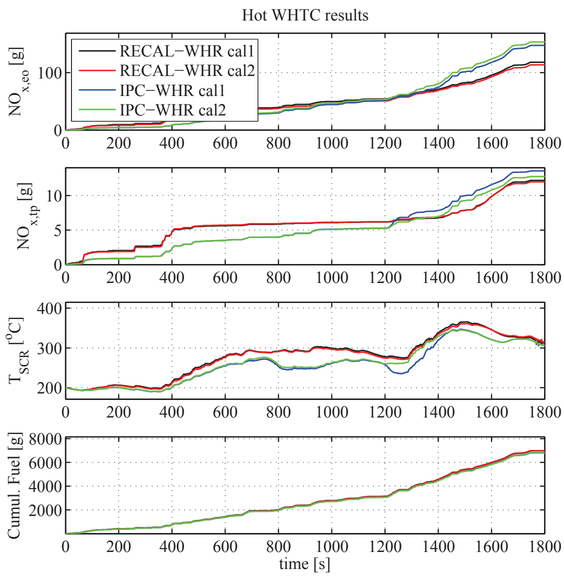

Fig. 12. Effect of WHR dynamics on performance-related, cumulative results

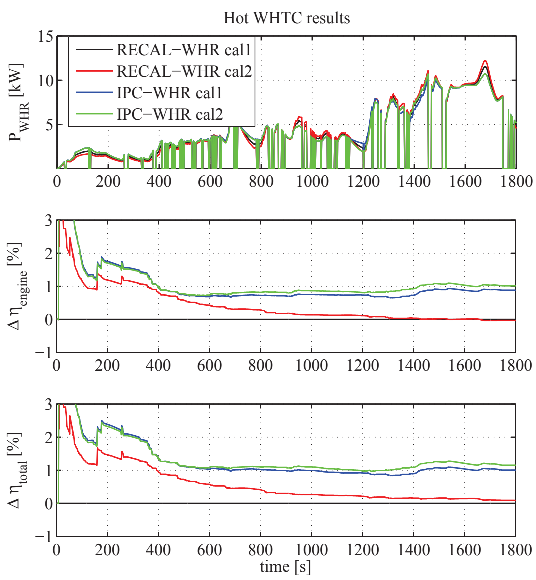

Fig. 13. Effect of WHR dynamics on efficiency-related results

the WHR power signal P_{WHR} is smoothed; effectively, P_{WHR} is reduced over the cycle. This reduced WHR output is compensated for by the torque management, Eq.(5), which results in increased fuel consumption and emissions. Furthermore, the operation of the actuator u_{WHR} is clearly visible: in accordance with Eq.(3), the WHR power delivery is shut off during motoring and idling conditions.

For both the recal-WHR and IPC-WHR case, the effect of the different strategies on emissions is illustrated in Figure 12. The IPC control strategy allows high engine out $NO_{x,eo}$ emissions when high SCR conversion efficiencies can be achieved (during the highway part), but it relies on low engine out $NO_{x,eo}$ emissions when T_{SCR} is too low. This so-called EGR-SCR balancing makes that the engine can be operated with higher cycle-averaged engine out $NO_{x,eo}$ emissions compared to the recal-WHR strategy. This holds for the cold as well as hot cycle, as shown Table 4. In addition, this situation adaptive behavior will enhance the performance robustness over various duty cycles. Differences in engine performance between IPC-WHR cal1 and cal2 are seen after 1200 [s], immediately after a considerable idling period. Due to different engine settings, the SCR catalyst temperature T_{SCR} for cal1 is significantly lower than for cal2, which leads to unacceptable cumulative tailpipe $NO_{x,tp}$ emissions. Also, the corresponding WHR power output P_{WHR} is affected, as illustrated in Figure 13.

Besides the effect of the different strategies on NO_x emissions, the impact on engine efficiency is examined. From Figure 13, it is learned that the WHR system delivers up to 12 [kW] for engine-assistance. The highest values are associated with the highway part of the WHTC. In order to make a distinction between effects related to modified engine operation and WHR power output, the engine and total efficiency are introduced, respectively:

$$\eta_{engine} = \frac{P_{engine}}{P_{fuel}}$$

$$\eta_{total} = \frac{P_{engine} + P_{WHR}}{P_{fuel}}$$

with $P_{fuel} = \dot{m}_f Q_{LHV}$ and lower heating value Q_{LHV} (in [MJ/kg]). The time-averaged efficiencies are plotted relative to the recal-WHR cal1 case. For both IPC cases, the largest contribution to efficiency improvement is due to modified engine operation: different EGR-valve and VTG settings. As illustrated in the upper figure, only a minor increase in P_{WHR} can be realized compared to the recal-WHR cal1 case; this results in small changes in engine torque $\tau_{e,req}$ and corresponding fuel consumption. For the recal-WHR cal2 case, the results over the hot WHTC are nearly identical to the cal1 results.

6. CONCLUSIONS AND FUTURE WORK

A supervisory controller for an Euro-VI engine with Waste Heat Recovery (WHR) system is presented. This controller is rooted in the IPC approach and integrates energy and emission management. From simulation results over a WHTC, it is concluded that a recalibration of the baseline engine controller is required to use the full CO_2 reduction

Table 4. Overview of WHTC results

Quantity	Control strategy			
	Recal-WHR		IPC-WHR	
	cal1	cal2	cal1	cal2
$NO_{x,eo}$[g/kWh]				
cold WHTC	3.67	3.54	4.37	4.56
hot WHTC	3.52	3.39	4.39	4.57
weighted WHTC	3.54	3.41	4.39	4.57
$NO_{x,tp}$[g/kWh]				
cold WHTC	0.71	0.68	0.55	0.55
hot WHTC	0.36	0.36	0.40	0.38
weighted WHTC	0.42	0.41	0.43	0.41
$NH_{3,max}[ppm]$				
WHTC	3.0	3.2	1.8	1.8
Costs [Euro]				
Fuel WHTC	9.36	9.35	9.14	9.11
AdBlue WHTC	0.11	0.10	0.14	0.15
PM WHTC	0.17	0.17	0.12	0.12
Total WHTC	9.64	9.62	9.40	9.37

potential of the WHR system. Furthermore, WHR dynamics have to be included in the control design: neglecting these dynamics leads to violation of the tailpipe $NO_{x,tp}$ limit. With the IPC strategy, a systematic approach is introduced, which optimizes the CO_2-NO_x tradeoff: additional 2.8% CO_2 reduction compared to the recalibrated baseline strategy (*Recal-WHR*).

Current research is dedicated to the development of a control-oriented WHR model. Furthermore, tests will be performed on an engine dynamometer to validate this model and to demonstrate the potential of the proposed controllers. For the IPC strategy, focus is on the robustness for different duty cycles. Alternative WHR system configurations (*e.g.*, expander not directly coupled to crank shaft) are also of interest.

REFERENCES

ACEA (2008). Vision 20-20. www.acea.be. ACEA Press Conference at the IAA 2008, Hanover, Germany.

ACEA (2011). Commercial vehicles and CO2. report, ACEA.

Bredel, E., Nickl, J., and Bartosch, S. (2011). Waste heat recovery in drive systems of today and tomorrow. *MTZ worldwide Edition*.

Cloudt, R. and Willems, F. (2011). Integrated Emission Management strategy for cost-optimal engine-aftertreatment operation. *SAE International Journal of Engines*, 4(1), 1784–1797.

EPA (2011). EPA and NHTSA adopt first-ever program to reduce greenhouse gas emissions and improve fuel efficiency of medium- and heavy-duty vehicles. Regulatory Announcement.

Geering, H. (2007). *Optimal control with engineering applications*. Springer Verlag.

Hounsham, S., Stobart, R., Cooke, A., and Childs, P. (2008). Energy recovery systems for engines. In *SAE World Congres, SAE paper 2008-01-0309*.

Howell, T., Gibble, J., and Tun, C. (2011). Development of an ORC system to improve HD truck fuel efficiency. In *Directions in Energy-efficiency and Emission Research DEER Conference*.

Kupper, F. (2012). *Integrated Powertrain Control for an Euro-VI heavy-duty diesel engine with Waste Heat Recovery system*. Master's thesis, Eindhoven University of Technology.

Nelson, C. (2009). Exhaust energy recovery. In *Directions in Energy-efficiency and Emission Research DEER Conference*.

Park, T., Teng, H., Hunter, G.L., van der Velde, B., and Klaver, J. (2011). A Rankine cycle system for recovering waste heat from HD diesel engines - Experimental results. In *SAE World Congres, SAE paper 2011-01-1337*.

Quoilin, S., Aumann, R., Grill, A., Schuster, A., Lemort, V., and Spliethoff, H. (2011). Dynamic modeling and optimal control strategy of waste heat recovery organic Rankine cycles. *J. Applied Energy*, 88(6), 2183–2190.

Willems, F. and Cloudt, R. (2011). Experimental demonstration of a new model-based SCR control strategy for cleaner heavy-duty diesel engines. *IEEE Transactions on Control Systems Technology*, 19(5), 1305–1313.

Willems, F. and Foster, D. (2009). Integrated Powertrain Control to meet future CO2 and Euro-6 emission targets for a diesel hybrid with SCR-deNOx system. In *IEEE Proc. of 2009 American Control Conference*, 3944–3949. St.Louis, MO, United States.

Willems, F., Kupper, F., and Cloudt, R. (2012). Integrated Powertrain Control for optimal CO2-NOx trade-off in an Euro-VI diesel engine with Waste Heat Recovery system. In *Proc. of 2012 American Control Conference*, 1296–1301. Montreal, Canada.